The Astrophysical Journal Letters, 811:L37 (5pp), 2015 October 1 doi:10.1088/2041-8205/811/2/L37

ASTEROSEISMIC MODELING OF 16 Cyg A & B USING THE COMPLETE *KEPLER* DATA SET

Travis S. Metcalfe[1], Orlagh L. Creevey[2,3], and Guy R. Davies[4]
[1] Space Science Institute, 4750 Walnut St. Suite 205, Boulder CO 80301, USA; travis@spacescience.org
[2] Laboratoire Lagrange, Université Côte d'Azur, Observatoire de la Côte d'Azur, CNRS, Blvd de l'Observatoire, CS 34229, F-06304 Nice cedex 4, France
[3] Institut d'Astrophysique Spatiale, CNRS, UMR 8617, Université Paris XI, Batiment 121, F-91405 Orsay Cedex, France
[4] School of Physics and Astronomy, University of Birmingham, Birmingham B15 2TT, UK
Received 2015 August 5; accepted 2015 September 16; published 2015 September 29

ABSTRACT

Asteroseismology of bright stars with well-determined properties from parallax measurements and interferometry can yield precise stellar ages and meaningful constraints on the composition. We substantiate this claim with an updated asteroseismic analysis of the solar-analog binary system 16 Cyg A & B using the complete 30-month data sets from the *Kepler* space telescope. An analysis with the Asteroseismic Modeling Portal, using all of the available constraints to model each star independently, yields the same age ($t = 7.0 \pm 0.3$ Gyr) and composition ($Z = 0.021 \pm 0.002$, $Y_i = 0.25 \pm 0.01$) for both stars, as expected for a binary system. We quantify the accuracy of the derived stellar properties by conducting a similar analysis of a *Kepler*-like data set for the Sun, and we investigate how the reliability of asteroseismic inference changes when fewer observational constraints are available or when different fitting methods are employed. We find that our estimates of the initial helium mass fraction are probably biased low by 0.02–0.03 from neglecting diffusion and settling of heavy elements, and we identify changes to our fitting method as the likely source of small shifts from our initial results in 2012. We conclude that in the best cases reliable stellar properties can be determined from asteroseismic analysis even without independent constraints on the radius and luminosity.

Key words: stars: individual (HD 186408, HD 186427) – stars: interiors – stars: oscillations – stars: solar-type

1. INTRODUCTION

Asteroseismology is emerging as a powerful technique to determine the ages and other properties of field stars (Metcalfe et al. 2014), including the parent stars of planetary systems (Silva Aguirre et al. 2015). During the nominal *Kepler* mission, the data analysis and modeling methods for asteroseismic inference matured substantially, and the techniques are now being applied to brighter stars and members of well-characterized clusters for the *K2* mission (Howell et al. 2014; Chaplin et al. 2015). These studies will ensure that automated methods to determine stellar properties are as reliable as possible prior to the collection of asteroseismic data for bright stars all around the sky with the Transiting Exoplanet Survey Satellite (TESS, Ricker et al. 2014).

The old solar analogs 16 Cyg A & B are among the brightest stars ($V \sim 6$) within the original *Kepler* field of view. Precise photometric measurements were obtained every 58.85 s almost continuously for 2.5 years, between 2010 September 23 and 2013 April 8 (quarters Q7–Q16). Metcalfe et al. (2012) conducted an initial asteroseismic analysis of 16 Cyg A & B using the first 3 months of *Kepler* data, identifying more than 40 oscillation modes in each star. The optimal models, derived by fitting the observations of each star independently, had the same age and initial composition within the uncertainties—as expected for the components of a binary system. These initial results bolstered our confidence in the reliability of asteroseismic techniques.

Since the original study by Metcalfe et al. (2012) the time series for 16 Cyg A & B has been extended by an order of magnitude, and radius constraints from interferometry are now available (White et al. 2013). The complete *Kepler* data sets have already been used to constrain the bulk helium abundances (Verma et al. 2014), and to determine rotation rates and inclinations (Davies et al. 2015) for both components. Using these new observational constraints, and applying the improved modeling methods developed over the past several years, the aim of this letter is to quantify the precision and accuracy of asteroseismic inferences for the bright targets that will be observed by future missions such as TESS and PLATO (Rauer et al. 2014).

In Section 2 we outline the previously published observations that we adopt for our analysis, including a photometric data set for the Sun degraded to *Kepler*-like precision. We summarize recent updates to our methods in Section 3, and we describe a new set of experiments using the Asteroseismic Modeling Portal (AMP, Metcalfe et al. 2009; Woitaszek et al. 2009) to probe the influence of different observational constraints and fitting methods. Finally, in Section 4 we discuss the precision and accuracy of the derived stellar properties for 16 Cyg A & B, using the solar results to identify any biases.

2. OBSERVATIONAL CONSTRAINTS

To update our asteroseismic analysis, we adopted the sets of frequencies published by Davies et al. (2015), including 54 and 56 oscillation modes for 16 Cyg A & B respectively. These frequency sets were extracted from the power spectra of 928 days of short-cadence observations with a duty cycle of 90.5%. Each set includes 15 consecutive orders for the radial ($l = 0$), dipole ($l = 1$) and quadrupole ($l = 2$) modes, as well as 9 and 11 octupole ($l = 3$) modes for 16 Cyg A & B respectively. Compared to the 3 months of data presented in Metcalfe et al. (2012), the longer time series analyzed by Davies et al. (2015) typically allowed the detection of 1–2 additional orders at lower and higher frequencies and improved the precision by a factor of 2–4 for previously detected modes, consistent with the expectations of Libbrecht (1992).

In addition to the frequencies, we adopted other observational constraints from spectroscopy, *Hipparcos* parallaxes

(van Leeuwen 2007), and interferometry. The spectroscopic constraints and luminosities were similar to those used by Metcalfe et al. (2012): $T_{\rm eff,A} = 5825 \pm 50$ K, $[M/H]_A = 0.10 \pm 0.09$, $T_{\rm eff,B} = 5750 \pm 50$ K, $[M/H]_B = 0.05 \pm 0.06$ (Ramírez et al. 2009), $L_A = 1.56 \pm 0.05\ L_\odot$ and $L_B = 1.27 \pm 0.04\ L_\odot$ (Metcalfe et al. 2012). Note that we adopted 3σ uncertainties on the spectroscopic metallicities to allow for potential systematic errors. Unlike the 2012 study, radius constraints are now available from the interferometric observations of White et al. (2013), who used the CHARA array (ten Brummelaar et al. 2005) with the PAVO beam combiner (Ireland et al. 2008). They found linear radii $R_A = 1.22 \pm 0.02\ R_\odot$ and $R_B = 1.12 \pm 0.02\ R_\odot$, which were combined with an asteroseismic scaling relation (Ulrich 1986) to obtain mass estimates $M_A = 1.07 \pm 0.05\,M_\odot$ and $M_B = 1.05 \pm 0.04\ M_\odot$. The radius estimates are independent of asteroseismology, so we adopt them as constraints for the modeling presented in Section 3. We note the mass estimates here only for comparison with our final results (see discussion in Section 4).

To assess any biases in our modeling, we adopted a photometric data set for the Sun that was used by Davies et al. (2015) for validation of their analysis methods. The solar data were obtained from the red channel of the VIRGO instrument (Fröhlich et al. 1995) on the *Solar and Heliospheric Observatory* (*SOHO*) satellite (Domingo et al. 1995) with white noise added to approximate the *Kepler* data for 16 Cyg A & B. The solar power spectrum was analyzed using the same methods that were used for 16 Cyg, and the extracted frequencies were chosen to include the same set of modes (relative to the frequency of maximum power) detected in 16 Cyg A. The resulting solar frequency errors are comparable to those obtained for 16 Cyg A, and all other observational constraints for the Sun were fixed at the known values with the same fractional errors as 16 Cyg A: $T_{\rm eff,\odot} = 5777 \pm 50$ K, $[M/H]_\odot = 0.00 \pm 0.09$, $L_\odot = 1.000 \pm 0.032$, and $R_\odot = 1.000 \pm 0.016$.

3. ASTEROSEISMIC MODELING

We used the observational constraints described in Section 2 to obtain the optimal stellar properties with AMP from various data sets and fitting methods. The AMP science code uses a parallel genetic algorithm (Metcalfe & Charbonneau 2003) to optimize the match between models produced by the Aarhus stellar evolution and pulsation codes (Christensen-Dalsgaard 2008a, 2008b) and a given set of observations. The models are configured to use the OPAL 2005 equation of state (Rogers & Nayfonov 2002) with opacities from OPAL (Iglesias & Rogers 1996) and Ferguson et al. (2005), and nuclear reaction rates from the NACRE collaboration (Angulo et al. 1999, 2005). Convection is treated using mixing-length theory (Böhm-Vitense 1958) without overshoot, while diffusion and settling of helium is treated with the prescription of Michaud & Proffitt (1993). The AMP software has been in development since 2004, and below we briefly outline its history to place the current modeling approach in context.

3.1. Updated Physics and Methods

The AMP 1.0 software (Metcalfe et al. 2009) reproduced the solar properties from Sun-as-a-star data, but we had more difficulty fitting the early asteroseismic observations from *Kepler* (Metcalfe et al. 2010). For AMP 1.1 (Mathur et al. 2012; Metcalfe et al. 2012) we used the statistical errors on each oscillation frequency to assign weights, rather than using a combination of statistical and systematic errors that gave lower weight to higher frequencies where so-called "surface effects" dominated. We also split our χ^2 quality metric into separate components for seismic and non-seismic observables, to prevent the many oscillation frequencies from overwhelming the relatively few and less precise spectroscopic constraints. For AMP 1.2 (Metcalfe et al. 2014) we updated the model physics to use the NACRE reaction rates (Angulo et al. 1999) instead of those from Bahcall et al. (1995) and the low-temperature opacities of Ferguson et al. (2005) instead of Alexander & Ferguson (1994). We also began fitting two sets of frequency ratios r_{010} and r_{02} (Roxburgh & Vorontsov 2003) in addition to the frequencies themselves, combining these three sets of observables with a set of spectroscopic and other constraints into an average χ^2 quality metric.

We have made several important updates to AMP for the results presented here. First, we implemented the revised rate for the $^{14}N + p$ reaction determined by the NACRE collaboration (Angulo et al. 2005). Second, we now use only the frequency ratios r_{010} and r_{02} (along with r_{13} for 16 Cyg A & B where the $l = 3$ modes are detected) rather than the individual frequencies for modeling. This allows us to avoid potential biases from applying an empirical correction for surface effects (e.g., Kjeldsen et al. 2008). The frequency ratios are insensitive to the near-surface layers by design, so they allow a direct comparison between observations and models without resorting to any ad hoc frequency corrections. The frequency ratios are also insensitive to line of sight Doppler velocity shifts (see Davies et al. 2014). Finally, we combine all of the observational constraints into a single χ^2 quality metric to facilitate the statistical interpretation of the results. The average χ^2 metric used in AMP 1.2 was designed to yield the optimal trade-off between complementary sets of constraints, but it complicated the determination of reliable uncertainties on the inferred stellar properties. We calculated the uncertainties in the same manner as described in Metcalfe et al. (2014), but using the single χ^2 value instead of an average χ^2 to determine the likelihood of each sampled model. The AMP 1.2 fitting method can optionally still be used, and we have implemented the scaled solar surface correction proposed by Christensen-Dalsgaard (2012) to help minimize any resulting biases. We demonstrate below that our results are largely insensitive to the particular choice of fitting method.

3.2. Results for 16 Cyg A & B and the Sun

We used AMP to investigate how the reliability of asteroseismic inference changes when various sets of observational constraints are adopted or when slightly different fitting methods are employed. The optimal asteroseismic properties of 16 Cyg A & B and the Sun for each case are listed in Table 1, and the variations are described below.

The most reliable properties, obtained by applying the updated fitting method described above to the complete set of observational constraints,[5] are shown in the first case labeled "all constraints" in Table 1 (AMP simulations 767, 768 and 766 for 16 Cyg A, 16 Cyg B and the Sun respectively). All

[5] The constraints used for each case are provided as an obs.dat file on the AMP website at http://amp.phys.au.dk.

Table 1
Properties of the Optimal Models Using Various Constraints and Fitting Methods

Case	$R/R_\odot$	$M/M_\odot$	$L/L_\odot$	t/Gyr	Z	Y_i	log g	AMP[a]
16 Cyg A (*Kepler*)								
1: all constraints	1.229 ± 0.008	1.08 ± 0.02	1.55 ± 0.07	7.07 ± 0.26	0.021 ± 0.002	0.25 ± 0.01	4.292 ± 0.003	767
2: without R	1.225 ± 0.008	1.07 ± 0.02	1.53 ± 0.07	7.15 ± 0.27	0.020 ± 0.002	0.25 ± 0.01	4.291 ± 0.002	773
3: without R, L	1.225 ± 0.007	1.07 ± 0.02	1.52 ± 0.07	7.12 ± 0.23	0.021 ± 0.001	0.25 ± 0.01	4.291 ± 0.002	776
4: fitting method	1.229 ± 0.007	1.08 ± 0.02	1.55 ± 0.06	7.07 ± 0.37	0.021 ± 0.002	0.25 ± 0.01	4.292 ± 0.002	770
5: surface term	1.229 ± 0.008	1.08 ± 0.02	1.55 ± 0.07	7.07 ± 0.34	0.021 ± 0.002	0.25 ± 0.01	4.292 ± 0.002	797
6: 3 months data	1.229 ± 0.008	1.08 ± 0.02	1.55 ± 0.07	6.99 ± 0.37	0.024 ± 0.002	0.26 ± 0.01	4.292 ± 0.003	778
16 Cyg B (*Kepler*)								
1: all constraints	1.116 ± 0.006	1.04 ± 0.02	1.25 ± 0.05	6.74 ± 0.24	0.022 ± 0.003	0.26 ± 0.01	4.359 ± 0.002	768
2: without R	1.116 ± 0.006	1.04 ± 0.02	1.25 ± 0.06	6.74 ± 0.23	0.022 ± 0.002	0.26 ± 0.01	4.359 ± 0.002	774
3: without R, L	1.116 ± 0.006	1.04 ± 0.02	1.24 ± 0.06	6.79 ± 0.19	0.022 ± 0.002	0.26 ± 0.01	4.359 ± 0.002	777
4: fitting method	1.116 ± 0.005	1.04 ± 0.01	1.25 ± 0.05	6.89 ± 0.28	0.020 ± 0.002	0.25 ± 0.01	4.359 ± 0.002	771
5: surface term	1.116 ± 0.006	1.04 ± 0.02	1.24 ± 0.05	6.96 ± 0.29	0.020 ± 0.002	0.25 ± 0.01	4.359 ± 0.002	798
6: 3 months data	1.113 ± 0.006	1.03 ± 0.02	1.25 ± 0.05	6.66 ± 0.27	0.022 ± 0.001	0.27 ± 0.01	4.358 ± 0.002	779
Sun (*SOHO*/VIRGO)								
1: all constraints	1.003 ± 0.006	1.01 ± 0.02	0.98 ± 0.04	4.62 ± 0.15	0.018 ± 0.002	0.26 ± 0.02	4.439 ± 0.002	766
2: without R	1.007 ± 0.006	1.02 ± 0.02	1.02 ± 0.04	4.53 ± 0.15	0.018 ± 0.002	0.26 ± 0.01	4.440 ± 0.002	772
3: without R, L	1.010 ± 0.005	1.03 ± 0.02	1.00 ± 0.04	4.58 ± 0.14	0.018 ± 0.001	0.25 ± 0.01	4.442 ± 0.002	775
4: fitting method	1.010 ± 0.007	1.03 ± 0.02	1.00 ± 0.04	4.52 ± 0.18	0.020 ± 0.003	0.25 ± 0.01	4.442 ± 0.002	769
5: surface term	1.003 ± 0.007	1.01 ± 0.02	1.00 ± 0.03	4.61 ± 0.18	0.018 ± 0.003	0.26 ± 0.02	4.439 ± 0.002	799
6: 3 months data	0.996 ± 0.010	0.99 ± 0.03	1.00 ± 0.04	4.77 ± 0.18	0.017 ± 0.001	0.27 ± 0.02	4.437 ± 0.004	800

Note.
[a] Comprehensive model output is available at http://amp.phys.au.dk/browse/simulation/###.

three models match the spectroscopic and other constraints with a reduced $\chi^2 < 1$. The quality of the match to the asteroseismic constraints for 16 Cyg A & B is illustrated in Figure 1 where the bottom panels show the match to the frequency ratios that were actually used as constraints for the modeling, while the top panels show the match to the frequencies after the scaled solar surface correction of Christensen-Dalsgaard (2012) has been applied to the raw model frequencies. All of the models that result from variations to the set of observational constraints and to the fitting methods yield comparable matches to both the asteroseismic and other constraints. The primary reason for exploring such variations is to quantify the absolute accuracy of the inferred stellar properties, and to assess the sensitivity of the results to details of the modeling strategy and data quality.

We can test the absolute accuracy of our results by eliminating the independent constraints on radius and luminosity to see whether the asteroseismic and spectroscopic constraints alone are sufficient to determine these properties. Interferometric radius constraints are available only for relatively nearby stars, so the second case (labeled "without R" in Table 1, AMP simulations 773, 774 and 772) removes this constraint from the χ^2 value that guides the search. For 16 Cyg A and the Sun this leads to small shifts within the quoted uncertainties for the optimal stellar properties, while only the uncertainties change for 16 Cyg B. Luminosity constraints are currently available for a small fraction of stars in the *Kepler* field, at least until parallaxes are released by the *Gaia* mission (Perryman et al. 2001). Parallaxes are also needed to convert the angular measurements from interferometry into a linear radius, so our third case (labeled "without R, L" in Table 1, AMP simulations 776, 777 and 775) omits both the radius and luminosity constraints. Again there are marginal shifts in the optimal stellar properties, insignificant for 16 Cyg A & B but slightly larger than the uncertainties for the solar radius and mass. In general, the reliability of asteroseismic inference seems to degrade more significantly for the Sun than for 16 Cyg A & B when the radius and luminosity constraints are not available.

Large samples of *Kepler* stars have previously been fit using slightly different methods to assess the quality of the match between the models and observations. To evaluate the impact of these differences on the inferred stellar properties, we fit the full set of constraints from the first case using two alternative modeling strategies. For the fourth case (labeled "fitting method" in Table 1, AMP simulations 770, 771 and 769) we used the AMP 1.2 fitting method (Metcalfe et al. 2014), which calculates an average χ^2 from four sets of observables including the frequencies corrected for surface effects with a solar-calibrated power law following Kjeldsen et al. (2008). Comparing the inferred stellar properties to the first case, 16 Cyg A yields slightly different uncertainties, 16 Cyg B is shifted within the uncertainties, and only the Sun shows marginally significant shifts in radius and mass. To probe the possible source of these biases, for the fifth case (labeled "surface term" in Table 1, AMP simulations 797, 798 and 799) we repeated the fourth case using the scaled solar surface correction of Christensen-Dalsgaard (2012) to replace the Kjeldsen et al. (2008) prescription. The differences were insignificant for 16 Cyg A & B, but for the Sun the alternative surface correction effectively eliminated the biases.

Finally, we examine the influence of using the longer asteroseismic time series by applying our updated fitting method to the original data sets for 16 Cyg A & B published in Metcalfe et al. (2012), along with a comparable 3-month solar data set from VIRGO. This final case (labeled "3 months data" in Table 1, AMP simulations 778, 779, and 800) should be compared to the second case "without R," since the original data sets did not include the radius constraints of White et al. (2013). For 16 Cyg A & B these two cases yield similar stellar

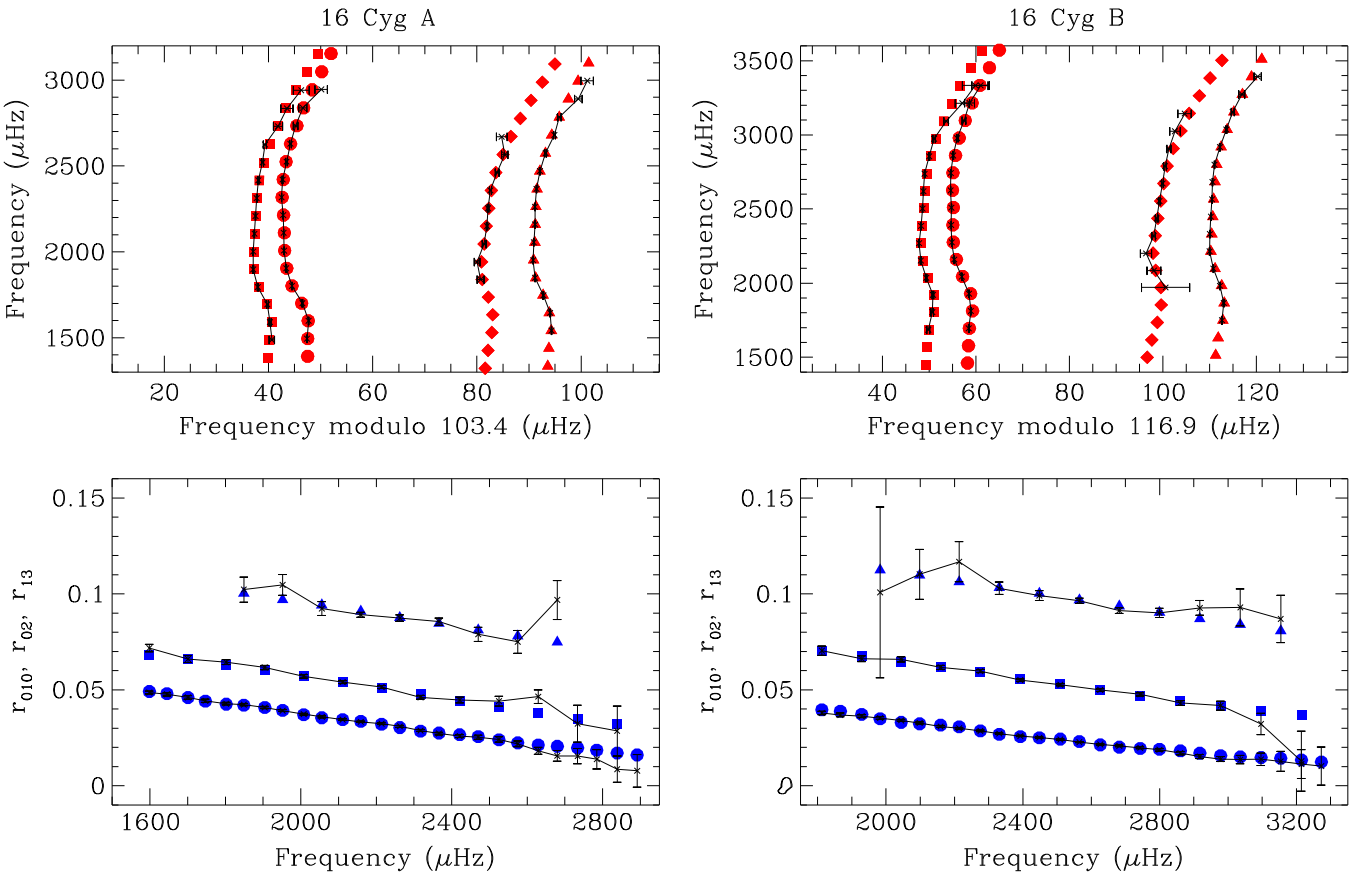

Figure 1. Échelle diagrams (top) and frequency ratios (bottom) for 16 Cyg A (left) and 16 Cyg B (right), with the observations shown as connected points with errors. Top panels: frequencies of the optimal models from AMP are shown using different symbols to indicate radial (circles), dipole (triangles), quadrupole (squares), and octupole (diamonds) oscillation modes. The scaled solar surface correction of Christensen-Dalsgaard (2012) was applied to all model frequencies for illustration. Bottom panels: frequency ratios r_{010} (circles), r_{02} (squares) and r_{13} (triangles) that were actually used as constraints for the modeling.

properties, indicating that differences relative to the Metcalfe et al. (2012) results can be attributed mostly to the updated model physics rather than the extended time series. For the Sun, the properties inferred from the shorter time series reproduce the solar radius, mass and luminosity more accurately. This seems to be a consequence of the fewer and lower-precision asteroseismic constraints, which gives the spectroscopic and other constraints more relative weight when all of the observations are combined into a single χ^2 quality metric.

4. DISCUSSION

We have determined precise asteroseismic properties for the solar-analog binary system 16 Cyg A & B, and we have quantified the accuracy of the results by varying the input constraints and fitting methods, and by applying the same techniques to the Sun. We obtain a radius precision of 0.6%, a mass precision of 2%, and an age precision of 3%. Our results for the Sun suggest that the systematic errors are smaller than or comparable to the statistical uncertainties, consistent with the conclusions of previous studies (e.g., Lebreton & Goupil 2014; Silva Aguirre et al. 2015). The radii and masses of 16 Cyg A & B are consistent with the estimates of White et al. (2013) from interferometry and scaling relations, but systematically lower than the original AMP results in Metcalfe et al. (2012). These differences persist when the radius constraint is omitted, or when the 2012 data set is analyzed with updated methods, suggesting that the use of frequency ratios as asteroseismic constraints is responsible. The luminosities of 16 Cyg A & B agree with the values derived by Metcalfe et al. (2012) from the *Hipparcos* parallaxes, though the best models for both components have luminosities slightly below the constraints. The solar radius, mass and luminosity are all recovered faithfully within the quoted precision, including small biases of $+0.3\%$ in radius, $+1\%$ in mass and -2% in luminosity. Note that results for significantly more massive or more evolved stars may not be as precise or accurate, even with comparable data quality.

Although we fit the observations of 16 Cyg A & B individually, the results for the two stars have a common age ($t = 7.0 \pm 0.3$ Gyr) and composition ($Z = 0.021 \pm 0.002$, $Y_i = 0.25 \pm 0.01$) within the uncertainties, as expected for the components of a binary system. The updated age is slightly older and more precise than the result presented in Metcalfe et al. (2012), and the updated methods in AMP now yield a consistent age for both components. The closest agreement between the two sets of models is obtained when using the AMP 1.2 fitting method with the scaled solar surface correction of Christensen-Dalsgaard (2012). The comparable fits to solar data agree with the seismic age of the Sun (4.60 ± 0.04 Gyr) as determined by Houdek & Gough (2011), with the ensemble of models in Table 1 showing a total age spread of only 0.25 Gyr (5%).

As with the original results of Metcalfe et al. (2012), we find values for the initial helium mass fraction that are systematically low compared to other estimates. Verma et al. (2014) used deviations from uniform frequency spacing in the oscillation modes to constrain the acoustic depths of the base of the convection zone (BCZ, τ_{cz}) and the helium ionization zone. The amplitude of deviations due to the latter source can be calibrated with models to determine the current helium mass fraction in the stellar envelope. The weighted average of three different methods using two different models for calibration yields $Y_s = 0.241 \pm 0.004$ for 16 Cyg A and $Y_s = 0.244 \pm 0.004$ for 16 Cyg B. In our models Y_s is systematically lower by 0.02–0.03, confirming that we are biased toward low initial helium. This issue had previously been identified by Gruberbauer et al. (2013) from Bayesian modeling of the 2012 data set for 16 Cyg A & B, and our results for the Sun show the same problem. We speculate that the bias toward low initial helium may be due to neglecting diffusion and settling of heavy elements, which is not stable under all conditions for the models used in AMP. We hope to remedy this issue with future development of AMP 2.0, which will use the MESA stellar evolution code (Paxton et al. 2011, 2013, 2015) and the GYRE pulsation code (Townsend & Teitler 2013).

An additional diagnostic of our best models is whether they agree with the convection zone depths derived by Verma et al. (2014). Although unrealistic surface boundary conditions in the models hinder direct comparisons, Mazumdar et al. (2014) suggest comparing the *fractional* acoustic radius of the BCZ from observations and models. The total acoustic radius of the star T_0 can be estimated from the mean frequency spacing of radial modes Δ_0 using $T_0 \sim 1/(2\Delta_0)$. The fractional acoustic radius of the BCZ is then $T_{BCZ}/T_0 = 1 - (\tau_{cz}/T_0)$. The comparable quantity for a model is obtained from a numerical integration of the inverse sound speed from the center of the model to the BCZ, relative to a full integration out to the photosphere. A weighted average of the values of T_{BCZ}/T_0 from three methods using the data in Tables 1 and 3 of Verma et al. (2014) gives 0.368 ± 0.012 for 16 Cyg A and 0.391 ± 0.028 for 16 Cyg B, while our best models yield 0.386 and 0.381 respectively—slightly above the constraint for 16 Cyg A ($+1.5\sigma$), but consistent for 16 Cyg B (-0.4σ). Future efforts should consider how to include the fractional acoustic radius of interior features as additional constraints for the modeling.

Automated asteroseismic modeling has advanced significantly in the past few years, and we are on track to take full advantage of the large data sets that will emerge from future missions like TESS (1–12 month time-series) and PLATO (5–36 months per field). The analysis presented in this Letter demonstrates that high precision and reasonable accuracy is possible for the brightest asteroseismic targets, with or without independent constraints on the radius and luminosity. It is also clear that our results are largely insensitive to fine details of the modeling strategy, but significant biases are possible when using simple power law corrections for surface effects and when neglecting diffusion and settling of heavy elements. Efforts are underway to define the character of these systematic errors across a broad range of stellar properties, and to minimize or correct the model deficiencies that contribute to the biases. We look forward to additional opportunities to demonstrate the reliability of asteroseismic properties using observations of cluster members, binary systems, and interferometric targets.

This work was supported by NASA grants NNX13AE91G and NNX15AF13G. Computational time at the Texas Advanced Computing Center was provided through XSEDE allocation TG-AST090107. G.R.D. acknowledges support from the UK Science and Technology Facilities Council (STFC).

REFERENCES

Alexander, D. R., & Ferguson, J. W. 1994, ApJ, 437, 879
Angulo, C., Arnould, M., Rayet, M., et al. 1999, NuPhA, 656, 3
Angulo, C., Champagne, A. E., & Trautvetter, H.-P. 2005, NuPhA, 758, 391
Bahcall, J. N., Pinsonneault, M. H., & Wasserburg, G. J. 1995, RvMP, 67, 781
Böhm-Vitense, E. 1958, ZAp, 46, 108
Chaplin, W. J., Lund, M. N., Handberg, R., et al. 2015, PASP, in press (arXiv:1507.01827)
Christensen-Dalsgaard, J. 2008a, Ap&SS, 316, 13
Christensen-Dalsgaard, J. 2008b, Ap&SS, 316, 113
Christensen-Dalsgaard, J. 2012, AN, 333, 914
Davies, G. R., Chaplin, W. J., Farr, W. M., et al. 2015, MNRAS, 446, 2959
Davies, G. R., Handberg, R., Miglio, A., et al. 2014, MNRAS, 445, L94
Domingo, V., Fleck, B., & Poland, A. I. 1995, SoPh, 162, 1
Ferguson, J. W., Alexander, D. R., Allard, F., et al. 2005, ApJ, 623, 585
Fröhlich, C., Romero, J., Roth, H., et al. 1995, SoPh, 162, 101
Gruberbauer, M., Guenther, D. B., MacLeod, K., & Kallinger, T. 2013, MNRAS, 435, 242
Houdek, G., & Gough, D. O. 2011, MNRAS, 418, 1217
Howell, S. B., Sobeck, C., Haas, M., et al. 2014, PASP, 126, 398
Iglesias, C. A., & Rogers, F. J. 1996, ApJ, 464, 943
Ireland, M. J., Mérand, A., ten Brummelaar, T. A., et al. 2008, Proc. SPIE, 7013, 701324
Kjeldsen, H., Bedding, T. R., & Christensen-Dalsgaard, J. 2008, ApJL, 683, L175
Lebreton, Y., & Goupil, M. J. 2014, A&A, 569, A21
Libbrecht, K. G. 1992, ApJ, 387, 712
Mathur, S., Metcalfe, T. S., Woitaszek, M., et al. 2012, ApJ, 749, 152
Mazumdar, A., Monteiro, M. J. P. F. G., Ballot, J., et al. 2014, ApJ, 782, 18
Metcalfe, T. S., Chaplin, W. J., Appourchaux, T., et al. 2012, ApJL, 748, L10
Metcalfe, T. S., & Charbonneau, P. 2003, JCoPh, 185, 176
Metcalfe, T. S., Creevey, O. L., & Christensen-Dalsgaard, J. 2009, ApJ, 699, 373
Metcalfe, T. S., Creevey, O. L., Doğan, G., et al. 2014, ApJS, 214, 27
Metcalfe, T. S., Monteiro, M. J. P. F. G., Thompson, M. J., et al. 2010, ApJ, 723, 1583
Michaud, G., & Proffitt, C. R. 1993, in IAU Coll. 137, Inside the Stars, Vol. 40, 246
Paxton, B., Bildsten, L., Dotter, A., et al. 2011, ApJS, 192, 3
Paxton, B., Cantiello, M., Arras, P., et al. 2013, ApJS, 208, 4
Paxton, B., Marchant, P., Schwab, J., et al. 2015, ApJS, 220, 15
Perryman, M. A. C., de Boer, K. S., Gilmore, G., et al. 2001, A&A, 369, 339
Ramírez, I., Meléndez, J., & Asplund, M. 2009, A&A, 508, L17
Rauer, H., Catala, C., Aerts, C., et al. 2014, ExA, 38, 249
Ricker, G. R., Winn, J. N., Vanderspek, R., et al. 2014, Proc. SPIE, 9143, 914320
Rogers, F. J., & Nayfonov, A. 2002, ApJ, 576, 1064
Roxburgh, I. W., & Vorontsov, S. V. 2003, A&A, 411, 215
Silva Aguirre, V., Davies, G. R., Basu, S., et al. 2015, MNRAS, 452, 2127
ten Brummelaar, T. A., McAlister, H. A., Ridgway, S. T., et al. 2005, ApJ, 628, 453
Townsend, R. H. D., & Teitler, S. A. 2013, MNRAS, 435, 3406
Ulrich, R. K. 1986, ApJL, 306, L37
van Leeuwen, F. 2007, A&A, 474, 653
Verma, K., Faria, J. P., Antia, H. M., et al. 2014, ApJ, 790, 138
White, T. R., Huber, D., Maestro, V., et al. 2013, MNRAS, 433, 1262
Woitaszek, M., Metcalfe, T., & Shorrock, I. 2009, in Proc. of the 5th Grid Computing Environments Workshop, 1, arXiv:1011.6332